

## PHYSICS WITH THE UPGRADED CERES DETECTOR\*

HARALD APPELSHÄUSER

for the CERES-Collaboration

Physikalisches Institut, Universität Heidelberg  
Philosophenweg 12, 69120 Heidelberg, Germany*(Received August 4, 1998)*

The possible occurrence of a phase transition from hadronic to quark matter and a related restoration of chiral symmetry have been predicted within the framework of QCD. On the experimental side the investigation of dilepton production in heavy ion collisions is of particular interest, because electromagnetic radiation escapes the reaction volume without final state interactions and, therefore, provides information about the early hot and dense stage of the reaction. The significant enhancement of the dilepton yield observed in S+Au and Pb+Au collisions at SPS energies cannot be explained without the inclusion of non-trivial modifications of the in-medium properties of the vector mesons. To discriminate between different theoretical approaches, an improvement of the experimental data in terms of mass resolution and statistics is needed. For this purpose, the CERES detector at the CERN-SPS will be upgraded with a radial drift TPC located downstream of the existing spectrometer.

PACS numbers: 25.75.-q

**1. Recent results from CERES/NA45**

The CERES spectrometer is dedicated to the measurement of low-mass  $e^+e^-$ -pairs in the midrapidity region. The experimental setup of the CERES detector during the Pb-beam runs in 1995 and 1996 consisted of two Ring-Imaging Cerenkov Counters (RICH-1 and RICH-2), providing electron identification with full azimuthal coverage for polar angles between  $8^\circ$  and  $15^\circ$ , two layers of silicon drift detectors (SiDC), located about 10 cm downstream of the target system, and a multi-wire proportional chamber with

---

\* Presented at the Meson'98 and Conference on the Structure of Meson, Baryon and Nuclei, Cracow, Poland, May 26–June 2, 1998.

pad-readout (PADC) downstream of RICH-2. The momentum was determined by the measurement of the azimuthal deflection of the charged particles in a magnetic field between RICH-1 and RICH-2. The combination of all detectors allowed to cope with the high track density in Pb-induced collisions and improved the momentum resolution by almost 50% as compared to the original setup, giving a mass resolution [2] of  $\Delta m/m=8\%$  in the  $\rho/\omega/\phi$ -mass region.

Results for the production of  $e^+e^-$ -pairs in 158 A GeV Pb+Au collisions have been published by the CERES-collaboration [2]. The experimental data correspond to the most central 35% of the geometric cross section. Comparing the data to the contribution of hadronic decays, extrapolated from independent nucleon–nucleon-collisions (*hadronic cocktail*), the measured dilepton yield is enhanced by a factor  $3.5 \pm 0.4(\text{stat.}) \pm 0.9(\text{syst.})$  in the mass range  $m_{ee}=0.2\text{--}2$  GeV/ $c^2$ . The enhancement is most prominent for masses between  $2m_\pi$  and the  $\rho/\omega$ -resonances. Below the two-pion threshold the data are consistent with expectations from hadronic sources, chiefly  $\gamma$ -conversions and  $\pi^0$ -Dalitz-decays. The dilepton yield relative to the charged particle multiplicity is quantitatively similar to that previously observed in 200 A GeV S+Au-collisions [3]. The same is true for the overall spectral shape, in particular the absence of any significant  $\rho/\omega$ -peak structure.

The enhancement in the mass range  $m_{ee}=0.2\text{--}0.6$  GeV/ $c^2$  in Pb+Au collisions is found to be most pronounced at low pair transverse momenta. This is demonstrated in Fig. 1, where the inclusive  $e^+e^-$  invariant mass spectrum is shown for small and large transverse momenta.

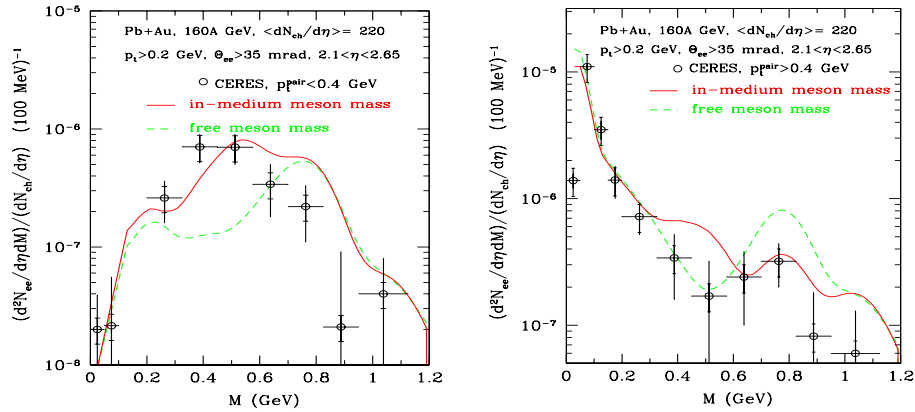


Fig. 1. CERES  $e^+e^-$  invariant mass spectrum in 158 AGeV Pb+Au collisions with  $p_t^{\text{pair}} < 0.4$  GeV/ $c$  (left panel) and  $p_t^{\text{pair}} > 0.4$  GeV/ $c$  (right panel), compared with transport calculations by G.Q. Li assuming Brown–Rho scaling (full curve) and free meson masses (dashed curve). The calculations are from [1].

## 2. Comparison to models

A large number of different theoretical approaches have shown that inclusion of  $\pi\pi$ -annihilation is not sufficient to explain the yield and spectral shape of dileptons produced in S+Au- and Pb+Au-collisions [4–7] as long as no in-medium modification of the properties of the vector mesons is taken into account; in fact the slope of the experimental data below the  $\rho/\omega$ -peak is even opposite to that of the model calculations. On the other hand, the experimental observations can be well described if medium modifications of the  $\rho$ -meson are taken into account. The Brown–Rho scaling approach [8], within which the  $\rho$ -meson mass drops linearly with baryon density, yields a very successful description of the data, as can be seen in Fig. 1. However, models that include in-medium properties related to hadronic rescattering processes (*collision broadening*) lead to a broadening rather than to a shift of the  $\rho$ -peak, and describe the data equally well [4, 6, 7]. It has been shown that in particular a strong coupling of the  $\rho$ -meson to the  $[N^*(1520)N^{-1}]^{1-}$  nucleon–hole state leads to an effective broadening and eventual disappearance of the  $\rho$ -pole [9], and again this approach yields a mass spectrum similar to the data [1]. In the context of in-medium modifications, it can be understood that the dilepton excess is largest at low  $p_t$ , since high  $p_t$  mesons have a higher probability to escape the medium and to decay in the vacuum.

Theoretical investigations have not yet conclusively answered the question to what extent the various approaches towards in-medium modifications are really conceptually different [1]. However, it has been pointed out that a distinction between some of the different models would be possible, if the mass resolution of the experimental data was significantly improved, as

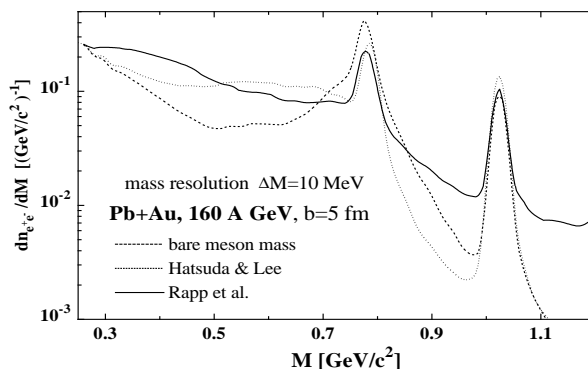


Fig. 2. Predicted  $e^+e^-$  invariant mass spectrum, calculated assuming different dilepton production scenarios and an experimental mass resolution of 10 MeV/ $c^2$  (Fig. from [7]).

shown in Fig. 2. In particular, between the  $\rho/\omega$  and the  $\phi$ -peaks as well as above the  $\phi$ -peak, the predictions for the dilepton yield, coming from two different scenarios, differ by almost one order of magnitude, after folding with a mass resolution of about  $10 \text{ MeV}/c^2$  [7].

### 3. The CERES-TPC

To improve the experimental information, the CERES-experiment will be upgraded by an additional tracking detector downstream of the existing spectrometer — a cylindrical Time Projection Chamber (TPC) with radial electric drift field [10] (see Fig. 3). The design of the TPC was constrained by the need to preserve the azimuthal symmetry of the existing spectrometer, matching the acceptance for polar angles between  $8^\circ$  and  $15^\circ$ .

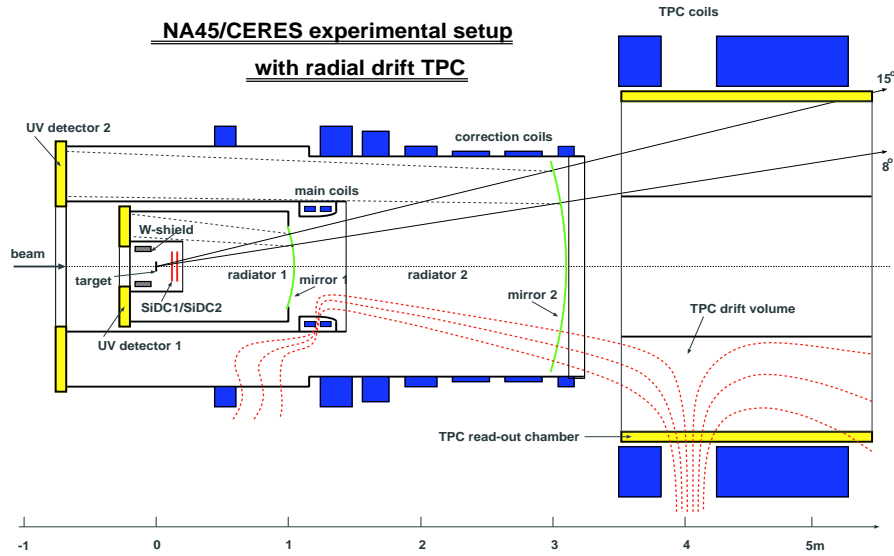


Fig. 3. CERES/NA45 setup, upgraded with a radial drift TPC.

The TPC has an active length of 2 m and an outer diameter of 2.6 m, and will be operated within a magnetic field, which is generated by two newly built warm coils. The currents (up to 4000 A) will run in opposite directions, resulting in a radial field component with maximum strength in the region between the two coils (indicated by the dashed lines in Fig. 3), deflecting the particles mainly in azimuthal direction. The bending power is 0.18 Tm at  $8^\circ$  and 0.38 Tm at  $15^\circ$ .

A charged particle traversing the counter gas volume of the TPC produces electron-ion-pairs along its trajectory. The electrons will drift in radial

direction along the lines of the electric drift field and finally reach one of the sixteen readout-chambers that are mounted in a cage-like aluminum structure and define the outer surface of the TPC (see Fig. 4). The electric drift field is provided by a cylindrical aluminum electrode with a diameter of 97.2 cm at a potential of typically  $-30$  kV, and by the cathode wire planes of the readout chambers at ground potential. In order to stabilize the drift field over the entire volume of the TPC, two voltage dividers enclose the counter gas volume at the endcaps of the TPC. The voltage dividers are made of  $50\text{ }\mu\text{m}$  Kapton foil with a Cu-coating of only 100–200 nm on both sides. A massive aluminum backplate and an outer aluminum cylinder provide the mechanical stability of the detector.

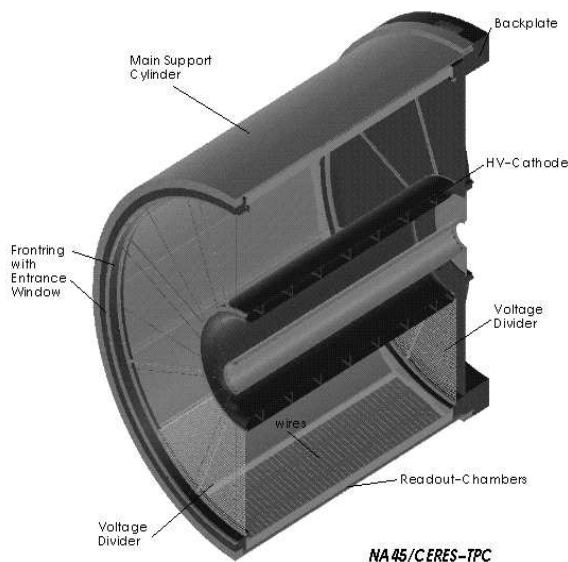


Fig. 4. Cross section through the CERES-TPC.

The readout chambers are conventional multi-wire proportional chambers with cathode pad-readout and have a size of  $2 \times 0.5\text{ m}^2$  each. Three planes of wires are running in azimuthal direction. The arriving charge cloud passes the gating and cathode wire planes and finally produces an avalanche close to the anode wires. The corresponding image charge typically spreads over two to three adjacent cathode pads in azimuthal direction, allowing precise determination of the arrival point of the electron cloud. The choice of chevron-type cathode pads turns out to be superior to the commonly used rectangular pads in terms of charge-sharing in azimuthal direction and minimization of differential non-linearities [11]. After a low-noise preamplification-shaping stage, the analog signals on each pad are sampled

in 256 time bins. The pulse height information is stored in a Switched-Capacitor Array (SCA), before it is digitized with an 8 bit ADC. The drift time information for each of the pad signals allows to determine the origin of the charge cloud in radial direction, thus providing a full three-dimensional coordinate measurement. The cathode pads are grouped in 20 rows in longitudinal (beam) direction, with 48 pads per row in each readout chamber. Hence, the TPC has a total of  $16 \times 20 \times 48 = 15360$  readout channels and provides a measurement of up to 20 space points per particle track.

The TPC will be operated with a Ne(80%)–CO<sub>2</sub>(20%) gas mixture. The choice of this mixture is a result of an optimization in terms of many different aspects, such as primary ionization, multiple Coulomb scattering, space charge properties, diffusion, and  $E \times B$ -effects. However, the low mobility of the gas mixture and the high electron attachment coefficient of O<sub>2</sub> require a relatively high drift field and low oxygen contamination. The expected position resolution using this gas mixture is 250–350  $\mu\text{m}$  in azimuthal and 400–500  $\mu\text{m}$  in radial direction, depending on the polar angle. This results in a mass resolution of  $\Delta m/m = 1.7\text{--}1.8\%$  in the  $\rho/\omega/\phi$ -mass region.

Over the past year, the TPC including read-out chambers, field cage and high voltage cathode has been assembled and first tests with laser and muon beams have been very encouraging: the voltage divider has been operated at  $-50$  kV, the measured O<sub>2</sub> concentration in the detector gas is below 4 ppm and preliminary results on the position resolution fall within the expected range.

#### 4. Plans for running

Fig. 5 shows the simulated dilepton mass spectrum, assuming the resolution quoted above and the unchanged natural line width. This study demonstrates that typically 20 thousands  $e^+e^-$ -pairs with  $m_{ee} = 0.2\text{--}2$  GeV/ $c^2$  are needed to fully benefit from the improved mass resolution. Together with an upgraded DAQ-performance of about 300 MB per 5 seconds extraction cycle (3 cycles per minute), this goal can be achieved in a typical yearly SPS beam period, when operating the TPC at a rate of about 1200 events per extraction cycle.

After engineering runs with  $p$ - and Pb-beams in the course of 1998, there will be a 158 AGeV Pb+Au production run in the fall of 2000. In addition, the CERN-SPS provides a 40 AGeV Pb-beam in the fall of 1999, which is of particular interest for the CERES collaboration. The lower bombarding energy results in different initial conditions of the reaction, in particular in lower energy and higher baryon density. Making use of the sensitivity of the dilepton production on the space-time evolution of the system and on its chemical composition, these data will help to further disentangle the different approaches to understand the properties of hot and dense matter.

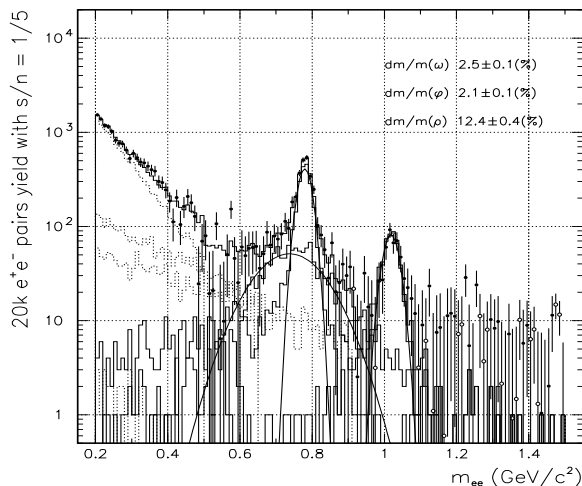


Fig. 5. Simulation of the hadronic cocktail, assuming the mass resolution of the upgraded CERES spectrometer and the natural line width.

## REFERENCES

- [1] G.E. Brown, G.Q. Li, R. Rapp, M. Rho, J. Wambach, preprint nucl-th/9806026 and private communication.
- [2] G. Agakichiev *et al.*, (CERES-Collaboration), *Phys. Lett.* **B422**, 405 (1998).
- [3] G. Agakichiev *et al.*, (CERES-Collaboration), *Phys. Rev. Lett.* **75**, 1272 (1995).
- [4] A. Drees, *Nucl. Phys.* **A630**, 449c (1998); I. Tserruya, *Nucl. Phys.*; J.P. Wurm, Proceedings of the ACTP Workshop on Hadron Properties in Medium, Seoul, October 1997, **A638** (1998), in print.
- [5] G.Q. Li, C.M. Ko, G. Brown, *Phys. Rev. Lett.* **75**, 4007 (1995); *Nucl. Phys.* **A606**, 568 (1996).
- [6] W. Cassing, W. Ehehalt, C.M. Ko, *Phys. Lett.* **B363**, 35 (1995); W. Cassing, W. Ehehalt, I. Kralik, *Phys. Lett.* **B377**, 5 (1996).
- [7] W. Cassing, E.L. Bratkovskaya, R. Rapp, J. Wambach, *Phys. Rev.* **C57**, 916 (1998).
- [8] G.E. Brown, M. Rho, *Phys. Rev. Lett.* **66**, 2720 (1991); T. Hatsuda, S.H. Lee, *Phys. Rev.* **C46**, R34 (1992).
- [9] R. Rapp, G. Chanfray, J. Wambach, *Nucl. Phys.* **A617**, 472 (1997).
- [10] Addendum to proposal SPSLC/P280: CERN/SPSLC 96-35/P280 Add.1.
- [11] B. Yu *et al.*, *IEEE Trans. Nucl. Sci.* **NS-38**, 454 (1991); W. Schmitz, CERES-Note 01-98 (1998).